Elucidating the role of water in collagen self assembly by isotopically modulating collagen hydration

Giulia Giubertoni[1,✉], Liru Feng[1], Kevin Klein[4,8], Guido Giannetti[1], Yeji Choi[5], Anouk van der Net[3], Gerard Castro-Linares[3], Federico Caporaletti[1,2], Dimitra Micha[7], Johannes Hunger[5], Antoine Deblais[2], Daniel Bonn[2], Andela Šarić[4], Ioana M. Ilie[1,6], Gijsje H. Koenderink[3], and Sander Woutersen[1]

[1]Van 't Hoff Institute for Molecular Sciences, University of Amsterdam, Amsterdam, The Netherlands
[2]Van der Waals-Zeeman Institute, Institute of Physics, University of Amsterdam, Amsterdam, The Netherlands
[3]Department of Bionanoscience, Kavli Institute of Nanoscience Delft, Delft University of Technology, Delft, The Netherlands
[4]Institute of Science and Technology Austria, Klosterneuburg, Austria
[5]Max Planck Institute for Polymer Research, Mainz, Germany
[6]Amsterdam Center for Multiscale Modeling (ACMM), University of Amsterdam, the Netherlands
[7]Amsterdam University Medical Centers (UMC), Vrije Universiteit Amsterdam, the Netherlands
[8]UCL, London, United Kingdom

Water is known to play an important role in collagen self assembly, but it is still largely unclear how water-collagen interactions influence the assembly process and determine the fibril network properties. Here, we use the H_2O/D_2O isotope effect on the hydrogen-bond strength in water to investigate the role of hydration in collagen self assembly. We dissolve collagen in H_2O and D_2O, and compare the growth kinetics and the structure of the collagen assemblies formed in these water isotopomers. Surprisingly, collagen assembly occurs ten times faster in D_2O than in H_2O, and collagen in D_2O self assembles into much thinner fibrils, that form a more inhomogeneous and softer network, with a fourfold reduction in elastic modulus compared to H_2O. Combining spectroscopic measurements with atomistic simulations, we show that collagen in D_2O is less hydrated than in H_2O. This partial dehydration lowers the enthalpic penalty for water removal and reorganization at the collagen-water interface, increasing the self assembly rate and the number of nucleation centers, leading to thinner fibrils and a softer network. Coarse-grained simulations show that the acceleration in the initial nucleation rate can be reproduced by the enhancement of electrostatic interactions, which appear to be crucial in determining the acceleration of the initial nucleation rate. These results show that water acts as a mediator between collagen monomers, by moderating their interactions so as to optimize the assembly process and, thus, the final network properties. We believe that isotopically modulating the hydration of proteins can be a valuable method to investigate the role of water in protein structural dynamics and protein self assembly.

Collagen | Hydration | Molecular structure | Mechanics
Correspondence: ***g.giubertoni@uva.nl***

Introduction

Collagen is the main component of connective tissues such as skin, arteries and bones, imparting to these tissues the mechanical integrity and properties required to ensure their biological functionality(1). The most abundant collagen type in our body is type I. The type I collagen chain contains around 1000 amino acids and is composed of Glycine(Gly)-Xaa-Yaa repeat units, where Xaa-Yaa are often Proline (Pro) and Hydroxy-proline (Hyp). Three polypeptide strands, adopting a left-handed polyproline II-type (PPII) conformation, further associate to form the typical triple helix, tropocollagen(2).Tropocollagens (collagen monomers) self assemble to form intermediate fibrillar structures (microfibrils) that further associate into fibrils with an ordered molecular packing structure that maximizes fibril strength(1). The significance of this packing process is clearly shown in connective-tissue diseases in which it is disturbed due to genetic defects in the collagen type I genes; as a result, the mechanical integrity of diverse tissue types is affected (3).

During the self assembly process, water interacts with and binds to collagen, thereby influencing the mechanical properties of the final network. Water is believed to control collagen properties, for instance, by influencing the structure and stability of the triple helix(4–7) and mediating collagen inter- and intra-molecular interactions(8, 9). In particular, the water layer surrounding the collagen monomers (hydration layer) has been suggested to create a repulsive interaction ("hydration force") between collagen molecules, arising from the reorganization of the hydration layer that is required for collagen molecules to approach each other closely (9, 10). Research on collagen hydration has focused mostly on the effect of co-solvents, such as ethanol, propanol or glycerol, on the swelling properties of reconstituted fibril films(11, 12). These solvents, however, differ significantly from water, and having very different molecular sizes and dielectric constants than water, they modify not only the collagen hydration but also many other properties. Despite the evident importance of hydration for the properties of collagen fibrils, the mechanism by which water impacts collagen assembly is still largely unclear.

In this work, we study the role of water-collagen interactions on collagen assembly by replacing water with heavy water (D_2O). The hydrogen bonds between D_2O molecules are stronger (by $\sim$10%) than the ones between H_2O molecules(13, 14). However, contrary to the solvents

used previously to investigate collagen hydration, H_2O and D_2O have the same electronic structure, and nearly identical molecular size and dielectric constant (78.06 and 78.37, respectively)(15). Hence, changing the isotopic composition of the water can be used to modulate collagen-water interactions, and so study their effect on the assembly process without affecting the electrostatic interactions due to changes in the solvent dielectric constants. A significant effect of D_2O on protein self assembly has been recently observed for α-synuclein (aS) and insulin (INS)(16, 17). In these studies, it was suggested that in D_2O specific folded structures are stabilized, accelerating (in the case of aS) or slowing down (in the case of INS) the assembly.

Here, we find that the assembly of collagen occurs ten times faster in D_2O than in H_2O. This acceleration is somewhat similar to that observed previously for aS(16), but must have a very different origin: collagen has a more stable native ordered structure than aS, and (unlike aS) no drastic refolding of the protein is required for initiating the fibrilization (this refolding being a rate-limiting step for the fibrilization of aS). By combining infrared spectroscopy with atomistic simulations, we find that the faster self assembly observed for collagen in D_2O is due to the lowering of the energetic penalty of water removal and reorganization at the water-collagen interface, resulting in the enhancement of the initial nucleation rate. Coarse-grained simulations show that the different assembly growth rate and structure in D_2O can be reproduced by enhancing the electrostatic interactions, which appear to be largely affected by the desolvation energy, and to be central elements into driving the initial nucleation. Our results thus suggest that water guides collagen assembly by slowing down the fibril nucleation by moderating the attractive (mostly electrostatic) interactions between collagen monomers through the creation of a desolvation energy barrier.

Results

Network and fibril: kinetics and structure. We first study the influence of the isotopic water composition on the kinetics of collagen self assembly and on the collagen structure at the fibril and network level. We investigate the self assembly kinetics of collagen in H_2O and D_2O by using turbidimetry, a standard method (18–21) that relies on the increase in light scattering as the collagen monomers aggregate into fibrils or fibers (inset of Fig.1A). Fig.1A shows the turbidity-time curves measured in heavy water and water at a collagen concentration of 0.1 mg/ml. Both turbidity profiles show the typical sigmoidal growth profile, characterized by a lag phase of near zero turbidity followed by a growth phase with rapidly increasing turbidity. During the lag time (t_{lag}), collagen aggregates grow primarily in length but little in diameter, forming nuclei which have little ability to scatter light. Subsequently, during the growth phase, the collagen monomers anchor onto collagen nuclei, forming fibrils that quickly grow in diameter and molecular weight at a specific growth rate (k_g). When the monomers are depleted, the plateau phase is reached ($t_{plateau}$) as the fibrils attain their mature state(21). The turbidity profiles show that D_2O samples fibrillate much faster than the H_2O samples, somewhat similar to α-synuclein in D_2O and H_2O(16). The t_{lag} and $t_{plateau}$ for collagen assembly are ten-fold shorter in H_2O than in D_2O, and k_g is one order of magnitude larger in D_2O with respect to H_2O. In addition, the final turbidity value, $\Delta\tau$, is reduced from 0.55 ± 0.07 to 0.39 ± 0.01 in D_2O, indicating that D_2O favors the formation of thinner collagen fibrils(22) (this will be further investigated below).

We then performed rheology measurements to monitor the time-dependence of the mechanical response of the collagen solution during self assembly. The time-dependent elastic and viscous moduli (G' and G'', respectively) of a 0.5 mg/ml collagen solution in H_2O and D_2O (Fig.1D) show that collagen gelates faster in D_2O as compared to H_2O, as the elastic modulus reaches its plateau value earlier, consistent with the turbidity measurements. Furthermore, the final elastic modulus in water is $\sim$400% larger in water than in heavy water, indicating that the network is much softer in D_2O. Rheological and turbidity experiments in mixed H_2O:D_2O (1:1 volume ratio) indicate that D_2O-induced changes are D_2O-concentration dependent, with a significant effect already when $\sim$50% of H_2O is replaced by D_2O (see SI, section "HDO Measurements" and Fig. S1-2). Additional frequency-sweep oscillatory rheology measurements reveal that the dynamics of the network relaxation is not influenced by the presence of D_2O (Fig. S2B).

To investigate the effects of heavy water on the collagen network and fibril, we used confocal microscopy in reflectance mode (CRM) to obtain images of the networks (Fig.2). In water, collagen networks are isotropic and exhibit fan-shaped bundles of fibrils and large pore spaces, similar to the microstructures observed for rat tail Type I collagen in previous studies(22, 23). By contrast, gelation in heavy water does not lead to bundling, and instead a uniform and dense distribution of thin fibers is observed. We then used transmission electron microscopy (TEM) to obtain high-resolution images of the collagen networks (Fig.2B). We find that in H_2O the network has much larger pore spaces between the collagen fibrils than in D_2O. Quantitative analysis of the TEM images reveals that the collagen fibrils formed in heavy water are much thinner (Fig.2C): the average fibril thickness is 132 ± 55 nm in H_2O [in agreement with ref. (22)] and 52 ± 18 nm in D_2O .

Water-collagen interactions. To understand the molecular origin of the differences in collagen-assembly kinetics and structure in D_2O and H_2O, we compare the structure and hydration of monomeric collagen (its triple-helix structure is shown schematically in Fig.3A) in H_2O and D_2O using infrared (IR), two-dimensional IR (2D-IR) and circular dichroism (CD) spectroscopy. IR and 2D-IR spectroscopy probe the local structure and solvation by studying the infrared absorption bands of amide I modes(26–28), whereas CD spectroscopy probes the helicity(29, 30) and the stability(31) of collagen.

In Fig.3B, we report the normalized IR spectra of the triple-helical collagen monomer dissolved in D_2O and H_2O recorded at a temperature of 23 °C. We observe two main

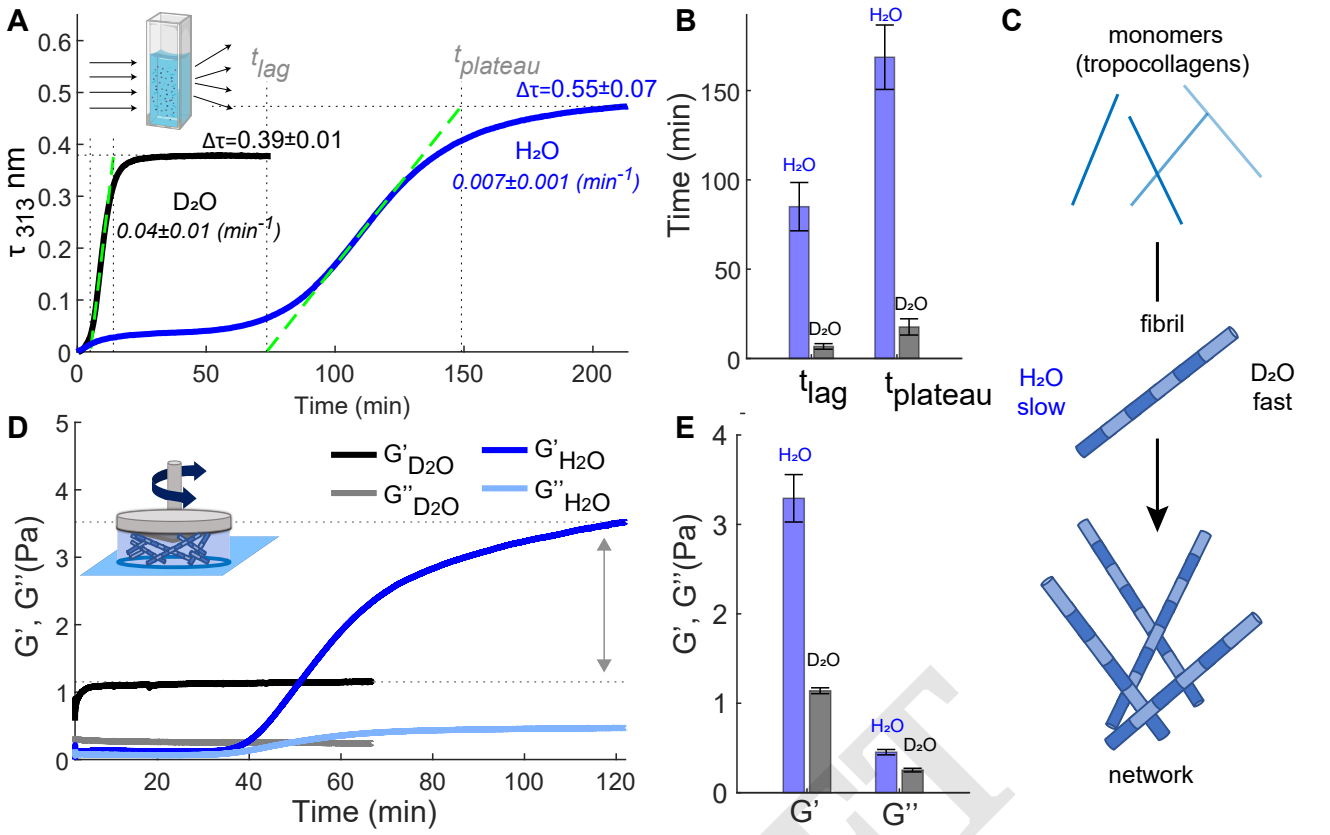

Fig. 1. Differences in collagen assembly kinetics and collagen-network elastic properties in H_2O and D_2O. **A**. Turbidity measurements for water and heavy water solutions containing Type I full-length collagen at a concentration of 0.1 mg/ml measured at a temperature of 23°C. Spectra were collected every 15 and 30 seconds for D_2O and H_2O experiments, respectively. **B**. Lag and plateau time values found for collagen fibrilization in H_2O and D_2O as described in SI. **C**. Schematic of collagen assembly in water and heavy water. **D**. Rheology measurement for water and heavy water solutions containing collagen at a concentration of 0.5 mg/ml. Measurements were conducted at a strain amplitude of 0.8%, an oscillation frequency of 0.5 Hz and temperature of 23°C. **E**. Elastic and viscous moduli after attaining the plateau level.

bands at 1635 cm^{-1} and 1660 cm^{-1}, in agreement with literature(25, 32–34) with the 1660 cm^{-1} band more intense in heavy water with respect to water. The low frequency band was previously assigned to the vibrations of carbonyl that are accessible and well-exposed to water(34); to verify this assignment we use 2D-IR spectroscopy, a technique that can provide direct information on the collagen hydration(27). In pump-probe 2D-IR spectroscopy, we use a tunable narrow-band pump pulse to excite molecular vibrations at a specific frequency ν_{pump}, and measure the pump-induced change in absorption ΔA at all frequencies using a broad-band probing pulse. Each vibrational mode of a molecule gives rise to a $+/-$ doublet on the diagonal(27). In the 2D-IR spectrum reported in Fig.3C, we observe two pairs of diagonal peaks at pump frequencies of 1635 cm^{-1} and 1660 cm^{-1}. The lineshapes of the two diagonal peaks differ significantly, with the 1660 cm^{-1} diagonal peak being more tilted with respect to the diagonal. The dependence of the 2D-IR response on the pump frequency is a measure of the inhomogeneous broadening of the IR band(27), which is due to a distribution of transition frequencies caused by solvent-protein interactions. The degree of inhomogeneity can be characterized by calculating the inverse value of the slope of the 2D-IR bleaches (central line slope or CLS)(35); and we find that the CLS values for the 1635 and for the 1660 cm^{-1} peaks are 0.7±0.15 and 0.35±0.11, respectively (values and errors represent the mean and standard errors obtained over 3 different measurements). The higher CLS value for the band at low frequency indicates a larger inhomogeneity, and thus a broader frequency distribution, than for the peak at 1660 cm^{-1}. The broader frequency distribution is due to interactions between functional groups and solvent molecules, indicating that the amide groups absorbing at 1635 cm^{-1} experience better solvation than the ones absorbing at 1660 cm^{-1}. We then fit the IR spectra in D_2O and H_2O (Fig.3B) by using Gaussian-shaped peaks (see SI and Fig.S4C-D for more details). We find that the area of the peak of the well solvent-exposed carbonyl decreases by ∼30% in intensity when collagen is dissolved in D_2O as compared to H_2O. This spectral difference [also observed in ref.(25)] was found to be independent of collagen concentration and amide H/D exchange (Fig. S4D-F). Furthermore, an increase in the ratio between less- and well-solvated carbonyl bands is observed in collagen fibril solutions when the fibrillation takes place in D_2O (Fig S4A); but also in collagen dissolved in H_2O (with the temperature set to 4°C to prevent fibrillation)(33).

We investigated whether the reduced hydration in D_2O influences the helicity of the collagen triple helix using CD spectroscopy. Fig.3D shows the CD spectra of collagen dissolved in water and heavy water at a concentration of 0.1 mg/ml.

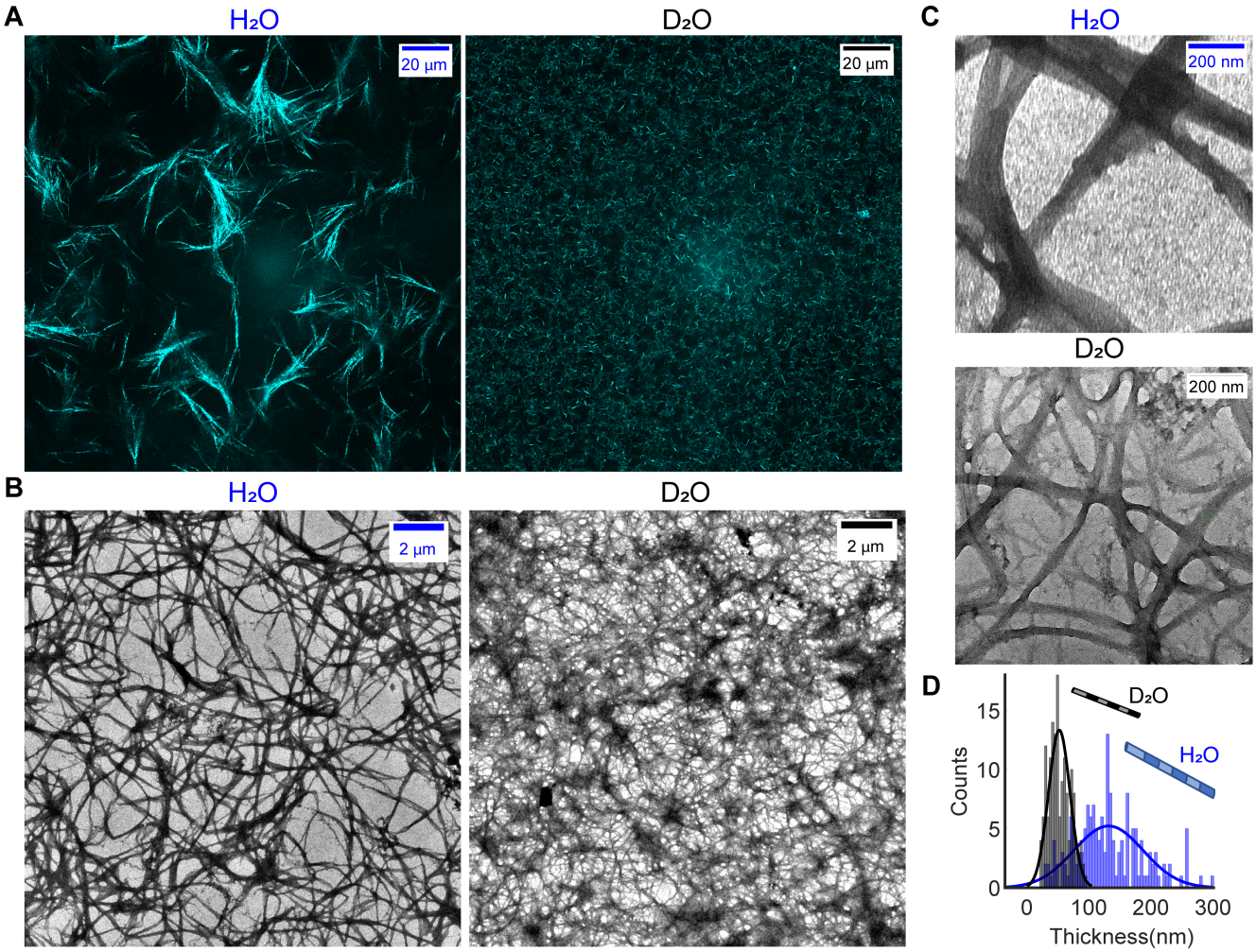

Fig. 2. Differences in the collagen fibril and network structures in H_2O and D_2O. **A**. Representative CRM images of the collagen network formed in water and heavy water at a concentration of 1 mg/ml. **B-C**. Representative TEM images of the collagen network formed in water and heavy water (the images in C are zoomed-in images of B). **D**. Distribution of the fibril thickness in H_2O and D_2O .

Both CD spectra have a minimum at 198 nm and a maximum at 220 nm, the typical spectral signatures of the collagen triple-helix.(29) To check whether the reduced solvation affects the collagen helicity, we calculate the ratio between the intensities of the maximum and the absolute of the minimum values, R_{pn} (an experimental criterion for triple-helicity)(30). We find identical ratios ($\sim$0.19) in H_2O and D_2O, indicating a similar helicity of collagen. In addition, we extracted the melting temperatures of the collagen triple helix from the temperature dependence of the CD spectra (see Fig.3E and SI for more details), resulting in 40 $\pm$1°C and 43$\pm$1°C in H_2O and D_2O, respectively. This result indicates that the collagen monomer has a less stable structure in H_2O than in D_2O, in agreement with previous studies on collagen-based peptides(31).

To validate the experimentally observed reduction in water-collagen interactions in D_2O compared to H_2O, we performed molecular dynamics simulations of the (Gly-Pro-Hyp) nonamer triple helix starting from its crystal structure (PDB ID: 3B0S(24), Fig.3A). Two sets of simulations were carried out in H_2O and D_2O at 300 K. In each case, five independent copies were run for a cumulated sampling time of 10 μs. The triple helices are structurally stable over the course of the simulations with an average root-mean-square deviation from the crystal structure of 2.4 $\pm$ 0.002 Å. The energetic analysis reveals that the total interaction energies between the nonamer and the solvent are less favorable in D_2O than in H_2O (-1818 ± 3 kcal/mol in D_2O and -1936 ± 2 kcal/mol in H_2O, Fig.3F). The reduction of water-protein interaction is also reflected in the smaller number of solvent-collagen hydrogen bonds in deuterated water (131$\pm$0.4) with respect in water (136$\pm$0.4), which confirms the experimentally observed reduced hydration in D_2O, and complements previous results on other biomolecules(36, 37). The total number of the total intramolecular energies(Fig.3G) and intramolecular hydrogen bonds are essentially identical, while the interaction with the ions is more favorable in D_2O (-223 ± 4 kcal/mol) than in H_2O (-158 ± 8 kcal/mol). The latter is probably an effect of the reduced hydration in D_2O as compared to H_2O. Thus, the molecular dynamics simulations show a reduction in water-collagen interactions in D_2O, leading to a less solvent-exposed and more stable protein struc-

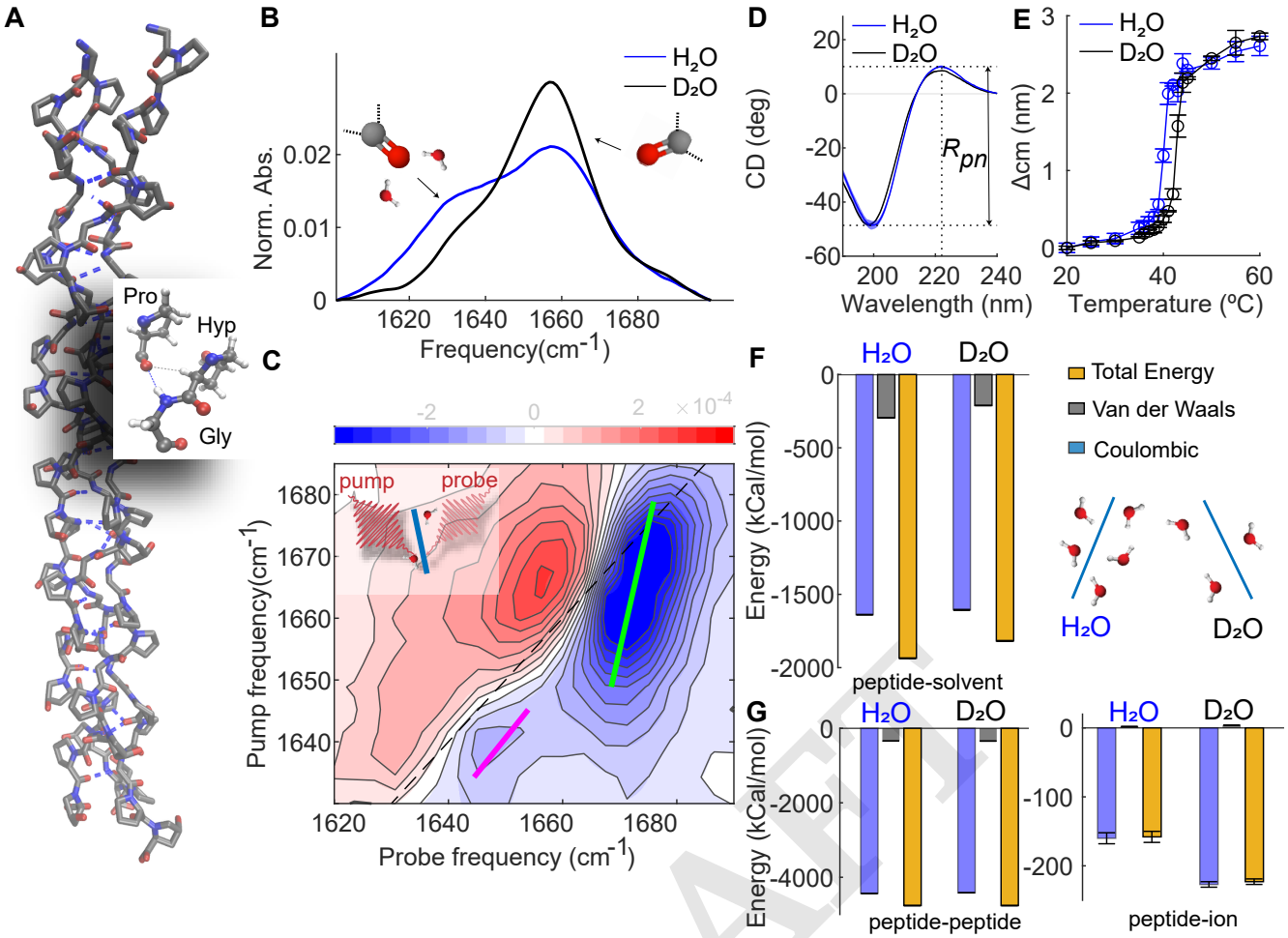

Fig. 3. Collagen is less hydrated in D_2O than in H_2O, but retains the same helicity. **A**. Crystal structure of the (Gly-Pro-Hyp) nonamer (PDB ID: 3B0S(24)). **B**. IR spectra of heavy water and water solutions containing Type I full-length collagen at a concentration of 2 mg/ml and 10 mg/ml, respectively, recorded at 23°C. Full IR spectra are shown in Fig.S3. The IR spectrum in D_2O was obtained using FTIR in transmission mode, in H_2O it was obtained by using FTIR in reflection mode (ATR-FTIR). In the latter case, because of the shorter optical path length, we use a higher collagen concentration to obtain a sufficient signal-to-noise ratio. The IR spectrum of collagen in water is not concentration dependent (see ref. (25) and Fig.S4). **C**. 2D-IR spectrum of a heavy water solution containing Type I full-length collagen at a concentration of 2 mg/ml recorded at a waiting time between pump and probe pulses of 1 ps. The blue contours represent a decrease in absorption ($\Delta A < 0$) due to depletion of the $\nu = 0$ state, and the red contours an increase in absorption ($\Delta A > 0$) due to the induced absorption of the $\nu = 1 \rightarrow 2$ transition. Colored lines in the 2D-IR spectrum represent the calculated central lines (See SI for more details). **D-E**. CD spectra and melting curves extracted from temperature-dependent CD measurements of Type I full-length collagen dissolved in water and heavy water at a concentration of 0.1 mg/ml, respectively (see SI for more details). **F** Interaction energies between the peptide and the solvent (D_2O, H_2O) molecules and schematic of collagen hydration in D_2O and H_2O. **G**. Intramolecular energies and energies between the peptide and the ions in D_2O and H_2O.

ture, as we observed in IR and 2D-IR measurements, without significantly altering the collagen helicity, as we observed in the CD measurements.

Collagen-collagen interactions. How can partial dehydration of collagen in D_2O modify the collagen-collagen interaction in such a way as to cause the observed changes in assembly kinetics and structure? To address this question, we perform coarse-grained molecular dynamics simulations using collagen-mimetic molecules. The assembly of collagen is known to be driven and regulated by an interplay between hydrophobic and electrostatic interactions(11, 38–45), and coarse-grained simulations have proven successful in revealing how this interplay controls the self assembly(46). To see which of these forces is most strongly influenced by the reduced hydration in D_2O, we systematically modify them in the simulations and see if we can reproduce the experimentally observed changes in collagen assembly rate and fibril structure. In the coarse-grained MD simulations, collagen molecules are described as elastic rods that carry a pattern of charges (Fig.4A). The rods can interact with each other via screened electrostatic interactions as well as via generic, hydrophobic attractions and have previously been shown to form clusters and collagen-like fibrils (46). Electrostatic interactions are modeled using a Debye-Hückel potential, while a Lennard-Jones potential is used for hydrophobic interactions. To study how the reduced hydration in D_2O can cause the observed changes in assembly rate and fibril structure, we vary the strength of electrostatic and hydrophobic interactions, and average the obtained results over ten independent simulation runs for each set of parameters. Snapshots of these simulations are shown in Fig.4B. The results (Fig.4C-D) show that increasing the hydrophobic interaction strength decreases the assembly rate and increases fibril diameter, the opposite of the experimentally observed trend. However, upon increasing the electrostatic interaction strength, the assembly rate is increased and fibril diameter is decreased, ex-

actly as is observed experimentally in D_2O (Figs. 1 and 2). These results indicate that the experimentally observed acceleration of assembly as well as the thinner fibrils in D_2O compared to H_2O can be effectively reproduced by enhancing electrostatic interactions, rather than by enhancing hydrophobic interactions.

Discussion

Our results show that changing the solvent from H_2O to D_2O causes a ten-fold acceleration of the collagen assembly (Fig. 1), and a dramatic structural change and softening of the final fibril network (Fig. 2). These differences become with increasing D_2O concentration, with a significant effect on the kinetics and mechanical properties already at a 1:1 ratio of H_2O:D_2O (Fig. S1-2). In the nucleation-growth mechanism of collagen self assembly, the fibril diameter is determined mainly during the nucleation step(47). Our coarse-grained simulations suggest that in D_2O more nucleation centers form due to the enhancement of electrostatic interactions between collagen monomers (Fig. 4). These nucleation centers compete with each other for the remaining collagen monomers, so that the increased attractive interaction in D_2O results in the thinner fibrils that are observed in the TEM images and the coarse-grained simulations. This is consistent with the thinner collagen fibrils formed at higher temperature, which also accelerates fibrilization(23). By combining (2D-)IR with CD and MD simulations we find that water-collagen interactions are reduced in D_2O, leading to a more stable and less water-bound structure, without altering the collagen helicity. These findings are consistent with previous studies which have shown that D_2O is a poorer protein solvent than H_2O, and that D_2O favors a less water-exposed but more stable protein structure(31, 48–57), affecting the assembly properties (16, 17, 58).

How can a reduction in collagen hydration affect the assembly process and the fibril structure so dramatically? For proteins to interact, the water molecules, which are tightly bound to the hydrophilic groups on the protein surface, have to be removed and reorganized, leading to a large energetic penalty (desolvation energy) for the protein assembly. Recently, it has been suggested that this desolvation energy plays a crucial role in the assembly of intrinsically-disordered proteins (IDP)(59): although the assembly into fibrils is thermodynamically favoured by the entropic gain in solvent release, the fibril nucleation is limited by the large desolvation energy. The initial self assembly rate can thus be increased in less hydrating conditions, resulting in a faster assembly. Our results indicate that the reduced hydration in D_2O affects the assembly process (and final fibril and network properties) in a similar manner, by lowering the desolvation energy barrier, which limits the initial nucleation. The coarse-grained simulations show that the acceleration in the initial nucleation rate can be reproduced by enhancement of the electrostatic interactions, suggesting that these interactions (rather than hydrophobic ones)are more sensitive to changes in the desolvation energy, and play a more important role in driving the initial nucleation. Although we believe that further experiments should be carried out to fully understand this last aspect, the role of hydrating water molecules in modulating electrostatic interactions has already reported for other proteins(59, 60), and a similar enhancement of the attractive interaction between collagen monomers as a result of a lower desolvation energy in D_2O seems plausible.

In earlier studies, it was already suggested that a short-range repulsive “hydration force” might be crucial for the structure and properties of collagen fibrils, and that the penalty associated to restructuring the tightly bound water molecules might prevent collagen molecules from coming too close to each other (9, 10, 12). However, so far this potential role of desolvation energy in collagen assembly was only indicated indirectly in experiments and simulations (11, 40, 41). The unique possibility of isotopically modulating the hydration while keeping the other solvent properties the same makes it possible to directly demonstrate the crucial role of the desolvation in collagen assembly. Our results indicate that water controls the mechanics of collagen networks by moderating attractive interactions between collagen monomers that guide the self assembly. In this way, water drives the formation of few initial nuclei rather than many competing ones, ensuring the cooperative nature of collagen self assembly. In the future, it would be interesting to determine whether specific regions in the collagen sequence, and if so which ones, are most important in establishing this mediating role of water. Furthermore, by exploiting the different hydration in D_2O and H_2O, we intend to probe this mediating role for collagen interactions with other tissue components, such as minerals in bones(61) and hyaluronic acid in cartilage(62).

Our findings provide new insights into how hydration modulates collagen properties to finely tune the mechanics of living tissues(63), and suggest new avenues toward the design of artificial collagen-based materials. Controllable and tunable macroscopic properties might be achieved by subtle changes in the solvent isotopic composition instead of alterating the chemical structure of a biomaterial’s building blocks. Finally, altered water-collagen interactions are believed to play a role in several age-related diseases(6, 64–66), and to partially contribute to tissue dysfunction in these disorders. It is well-known that genetic defects in the collagen type I genes COL1A1 and COL1A2 can cause osteogenesis imperfecta, Caffey disease and Ehlers-Danlos syndrome with a distinct bone or skin pathology, but our limited knowledge of the collagen folding hierarchy and its tissue-specific interfering factors set us still far from comprehending the mechanisms leading to such hyperostosis or fragility of bones, skin or blood vessels(67–69). The results presented here show that collagen hydration modulates the assembly rate and diameter of fibrils, which are also impacted in these diseases(70–72). It is therefore not unlikely that modified hydration may exacerbate the molecular defects of collagen type I (i.e. excessive posttranslational modification, misfolding) in determining the phenotypic outcome. We hope that further studies will give insight in the way that water distribution influences collagen quality, and how this might potentially be used for therapeutic purposes(73).

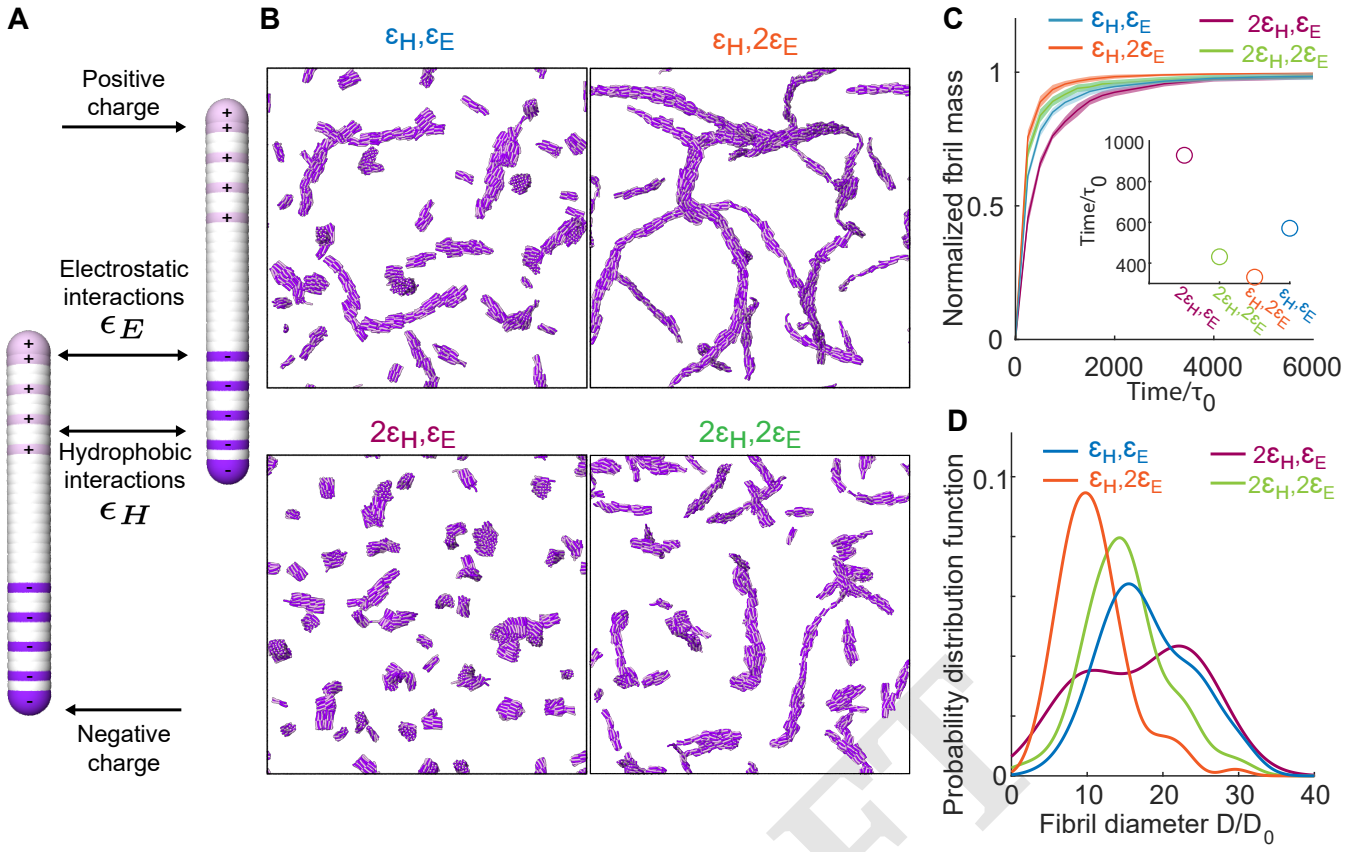

Fig. 4. Coarse-grained simulations can qualitatively reproduce the differences in collagen fibril and network structure in H_2O and D_2O. **A**. The collagen-mimetic molecules are simulated as elastic rods made of overlapping beads. The beads carry charges as indicated (positive are pink, negative are purple, and white is neutral). On top of these electrostatic interactions, all the beads between different molecules interact via generic hydrophobic interactions. **B**. Simulation snapshots of the equilibrated system for different combinations of electrostatic and hydrophobic interactions ($\epsilon_H = 0.05kT$, $\epsilon_E = 5kT$). **C**. Normalized fibril mass as a function of simulation time. The inset shows the time at which the assembled mass reaches 80% of the total monomer mass, where τ_0 is the MD unit of time. **D**. Probability distribution function of the fibril diameter D normalized by the smallest measured fibril diameter D_0.

Conclusion

We have shown that changing the solvent from H_2O to D_2O induces a tenfold acceleration of collagen assembly, and leads to thinner fibrils and a much softer collagen network, with significant effects already observable when 50% of H_2O is replaced by D_2O. By combining spectroscopy with molecular dynamics simulations, we have found that collagen in D_2O is less hydrated than in H_2O, and that it adopts a less water-exposed and more stable structure without altering its helicity. Our results indicate that the kinetic and structural changes originate from a lower energetic penalty for water removal and water reorganization at the collagen surface in D_2O, and coarse-grained simulations suggest that this desolvation energy influences mostly electrostatic interactions, which appear to be crucial in determining the nucleation rate. Our results directly demonstrate the role of hydration in collagen self assembly: the water layer surrounding the collagen acts as a mediator, moderating collagen-collagen interactions in order to slow down the assembly so as to optimize the final network properties.

Material and Methods

Sample preparation. Lyophilized collagen containing telopeptides (Type I collagen from rat tail tendon, Roche cat. no. 11179179001) was purchased from Sigma Aldrich. Deuterated materials used are: D_2O (deuterium oxide; Sigma-Aldrich, no. 151882-25G); Acetic acid-d_4 (Sigma-Aldrich, no. 233315-5G); NaOD (sodium deuteroxide; Sigma-Aldrich, no. 372072-10G). Collagen was dissolved in water, heavy water or 1:1 water:heavy water solutions containing 0.1 or 0.2% (v/v) of acetic acid (Emsure, no. 1000632500). The collagen was dissolved to obtain a final concentration of 0.2 mg/ml (for turbidity/CD measurements), 1 mg/ml (for rheology measurements) and 2 mg/ml or 10 mg/ml (for (2D-)IR measurements in heavy water and water, respectively), and stored at 4°C for at least 4 days before usage ensuring collagen is fully dissolved. All collagen samples were prepared on ice to prevent early self assembly and the self assembly was initiated by neutralizing acidic collagen solutions. First, weighing collagen in an Eppendorf tube and subsequently adding an equal volume of customized buffer solution to obtained a final pH of 7.3-7.5 and ionic strength I = 0.17 M. The customized buffer solution is made of Milli-Q water, 10× PBS (made with phosphate buffered saline tablet; VWR, no. E404-100TABS) solution, and 0.1 M NaOH (made with 1M sodium hydroxide solution; Honeywell Fluka, no. 319511-500ML). The customized buffer solution contained a fraction of 20% of PBS, whereas the Milli-Q:NaOH is 60%:20% or

40%:40%, depending on the initial acetic acid concentration. The pH of all the collagen solutions were measured by using a pH-meter (Thermo Scientific, Orion 2 Star) that was calibrated for measuring the pH in H_2O solutions instead of D_2O solutions. The measured pH^* of a D_2O solution was transformed to the pH value by using the following equation: $pH = (pH^* + 0.4) \cdot 0.929$ (74).

Infrared Spectroscopy. For IR-measurements of heavy water solutions, sample containing collagen at a concentration of 2 mg/ml was placed in a circular sample cell composed by two CaF_2 windows separated by a 100 μm spacer. Measurements were done in transmission mode using a Bruker Vertex 70. Per measurement, 32 scans were made, with a spectral resolution of 2 cm^{-1}. The temperature was kept at 23°C using a temperature controller (Julabo, TopTech F32-ME). The frequency range was from 7000 cm^{-1} to 400 cm^{-1}. For IR-measurements of water solutions, sample containing collagen at a concentration of 10 mg/ml (or 5 mg/ml) was measured in reflection mode using a PerkinElmer Frontier FT-IR spectrometer fitted with a Pike GladiATR module equipped with a diamond ATR-crystal (ø = 3 mm). Spectra were averaged over 20 scans. Temperature was maintained at room temperature by using a built-in heating/cooling plate. The spectrum of the solvent was subtracted to obtain the individual spectrum of the collagen.

Two-dimensional infrared spectroscopy. A detailed description of the setup used to measure the 2DIR spectra can be found in ref. 75. Briefly, pulses of wavelength 800 nm and with a 40 fs duration are generated by using a Ti:sapphire oscillator, and further amplified by using a Ti:sapphire regenerative amplifier to obtain 800 nm pulses at 1 kHz repetition rate. These pulses are converted in an optical parametric amplifier to obtain mid-IR pulses (∼20 μJ, ∼6100 nm) that has a spectral full width at half max (FWHM) of 150 cm^{-1}. The beam is split into a probe and reference beam (each 5%), and a pump beam (90%) that is aligned through a Fabry-Pérot interferometer. The pump and probe beams are overlapped in the sample in an ∼250-μm focus. The transmitted spectra of the probe (T) and reference (T_0) beams with pump on and off are recorded after dispersion by an Oriel MS260i spectrograph (Newport, Irvine, CA) onto a 2×32-pixel mercury cadmium telluride (MCT) array. The probe spectrum is normalized to the reference spectrum to compensate for pulse-to-pulse energy fluctuations. The 2DIR signal is obtained by subtracting the probe absorptions in the presence and absence of the pump pulse.

Circular dichroism. CD spectra were recorded with a JASCO CD spectrometer (Model: J-1500-150) in the far-UV at wavelengths, λ, ranging from 180 nm to 260 nm to obtain information on the secondary structure of the proteins. Data were recorded with a data pitch of 0.2 nm, a scan speed of 20 nm/min, a digital integration time of 0.5 s, and an optical path length of 1 mm. Spectra were smoothened using the Savitzky-Golay filter built-in in the spectrometer software. Temperature-dependent measurements were performed at temperatures ranging from 20 °C to 60 °C at increments of 5 °C with an equilibration time of 4 min. At 35-45 °C smaller increments of 1 °C were used with 8 min equilibration time. From each experiment the spectrum of the buffer was subtracted and the results of the three experiments were averaged for the final analysis.

Turbidity. The kinetics study of collagen self assembly was performed on a UV-Vis spectrophotometer (Agilent Technologies, Cary 8453). Neutralized cold collagen solutions were pipetted into plastic cuvettes (Brand, UV-Cuvette micro, no. 759220), which were quickly sealed with a cover to avoid evaporation and H/D isotopic exchange and subsequently placed in the water-jacked cuvette holder. Measurements were performed at 23 °C. Spectra were recorded every 15 s and 60 s after neutralization for heavy water and water samples, respectively. The spectrum of the respective solvent was used as a background. As collagen self assembly proceeded, the absorbance at a wavelength of 313 nm (A_{313}) were recorded as a function of time. Increase of A_{313} over time during collagen self assembly represents an increase in scattering. The absorbance readings were converted into turbidity values (τ) by using the relation: $\tau = A_{313} \cdot ln10$.

Rheology. Rheology study of collagen was performed with a stress-controlled rheometer (Anton Paar, Physica MCR 302), equipped with a cone-plate geometry (50 mm diameter, 1° cone angle, 100 μm gap). The bottom plate temperature was controlled using a Peltier element. Neutralized cold collagen solutions at a concentration of 1.25 mg/ml (experiments shown in SI) or 0.5 mg/ml (experiments shown in the main text) were pipetted onto the plate, and the cone was immediately lowered to the measuring position. We used a thin layer of low viscosity mineral oil (Sigma-Aldrich, no. 330760-1L) around the sample to prevent solvent evaporation and H/D isotopic exchange. Within ∼2 min the oscillatory rheology measurement was started.

CRM. To prepare collagen samples for CRM measurements, we used the protocol described in ref.(62) Briefly, neutralized cold collagen solution was pipetted into the customized sample holder, composed of two coverslips and the adhesive silicone isolator (Thermo Fisher Scientific, Press-to-Seal silicone isolator) in between. The coverslips were cleaned beforehand with isopropanol and Milli-Q water and dried by nitrogen flushing. The sample holder was then immediately placed into a petri dish and sealed by parafilm to prevent solvent evaporation and H/D isotopic exchange. Collagen at a concentration of 1 mg/ ml was left to polymerize at 23°C. Both water and heavy water samples were measured after at least 150 min at 23°C from neutralization to attain full network formation. The equilibrium collagen network images were taken by an inverted confocal laser scanning microscope (Leica Stellaris 8 platform) equipped with a 63x, NA = 1.30 glycerol-immersion objective (Leica), a (supercontinuum) white light laser with laser line 488 nm for illumination and the reflected light was dectected with silicon multi-pixel photon counter (Leica, Power HyD-S) detector. Glycerol (Leica, ISO 836) was used for objective immersion.

TEM. To prepare collagen samples for TEM measurements, we used the protocol described in ref.(76). Briefly, after neutralization, fibril assembly was initiated by placing the samples in a closed container (comprised of the cap of a closed Eppendorf tube placed upside down) for at least 150 minutes. The collagen fibrils were transferred to glow-discharged electron microscopy grid by peeling off the collagen gel drop surface with the grid (purchased from QuantiFoil, C support Cu400), which was left on the collagen surface between 1 to 12 hours. The sample was then washed 1 or times by placing a drop of milliQ water and blotting the drop without completely drying the grid. Finally, the sample was stained by adding a drop of 2% uranyl acetate and blotting it to dryness. TEM images were analyzed by using ImageJ, which is an image analysis and open source software(77). After scale calibration, thickness of the fibrils was calculated by taking the width of different fibrils in at least 4 different images of 4 different samples for a total of 150 measured thickness points. Width measurements were taken from the non-smoothed image by manually drawing a line perpendicular to the long axis of the bundle or the filament between the edges of the fibril. The edges were determined as the location where the darkened region produced by the defocus halo starts.

Molecular dynamics simulations. The crystal structure of

collagen-mimetic peptides composed of showing nine Gly-Pro-Hyp repeats (PDB ID: 3B0S (24)) was used as starting conformation. Two sets of simulations of the collagen triple helix {Gly-Pro-Hyp}$_9$ were carried out in water and heavy water at 300 K, cumulating 10 μs (5x2μs runs). All simulations were run using the GROMACS 2020.4 software package (78, 79), the CHARMM36m forcefield (80) and explicit solvent molecules, *i.e.* TIP3P for water and modified TIP3P-HW for heavy water (81).

Each collagen triple helix was solvated in a cubic box (12 nm per edge), with TIP3P (82) or TIP3P-HW (81) water molecules, to which 140 mM NaCl were added to mimic experimental conditions. The N- and C- termini were uncapped. Periodic boundary conditions were applied and the time step was fixed to 2 fs. Following the steepest descent minimization, the system were first equilibrated under constant pressure for 5 ns, with position restraints applied on the heavy atoms of the protein, followed by 5 ns NPT equilibration in absence of restraints. The temperature and the pressure were mantained constant at 300 K and 1 atm, respectively by using the modified Berendsen thermostat (0.1 ps coupling) (83) and Berendsen barostat (2 ps coupling) (84). The production simulations were performed in the NVT ensemble in absence of restraints. The short range interactions were cut-off beyond distances of 1.2 nm, and the potential smoothly decays to zero using the Verlet cut-off scheme. The Particle Mesh Ewald (PME) technique (85) was employed (cubic interpolation order, real space cut-off of 1.2 nm and grid spacing of 0.16 nm) to compute the long range electrostatic interactions.

Coarse grained molecular simulations. Our model is based on the "D-mimetic" molecule, which is a synthetic collagen-mimetic molecule, that has been shown to self-assemble into collagen-like fibrils (46, 86). Since this D-mimetic protein consists of 36 amino acids only, our molecule consists of 36 beads that are arranged into a linear chain. With σ being the MD unit of length, each of these beads measures $r = 1.12\sigma$ in diameter and is in contact with its direct neighbors via a harmonic bond $E = \kappa_{\rm bond}(r - r_0)^2$, where $\kappa_{\rm bond} = 500kT/\sigma^2$ is the bond strength and $r_0 = 0.255\sigma$ is the equilibrium distance. This results in a molecule length of $l = 10\sigma$ and consequently, $\sigma = 1$ nm, because the D-mimetic peptide has a length of 10 nm. We use an angular potential $E = \kappa_{\rm angle}(\theta - \theta_0)^2$ that acts between three neighboring beads to define the rigidity of our molecule, where $\kappa_{\rm angle} = 50kT$ controls the molecular rigidity and $\theta_0 = \pi$ is the equilibrium angle. Additionally, all beads carry a unit charge with respect to the charge distribution of the D-mimetic molecule, as shown in Fig. 4A in the main text. All the beads on different molecules are able to interact with each other via a generic, hydrophobic potential described by a cut-and-shifted Lennard-Jones potential $E_{\rm LJ} = 4\epsilon_{\rm H}\left[(\sigma/r)^{12} - (\sigma/r)^6\right] + E^{\rm LJ}_{\rm shift}$, if two interacting beads are at a distance $r < r_c = 2\sigma$, and is 0 otherwise, $\epsilon_{\rm H}$ is the strength of nonspecific or hydrophobic interactions , which is one of our control parameters. Furthermore, two charged beads i, j are able to interact with each other via a cut-and-shifted screened electrostatic potential (DLVO) $E_{\rm DLVO} = (\epsilon_{\rm E} q_i q_j/r)\exp(-\kappa r) + E^{\rm DLVO}_{\rm shift}$, if the two beads are at a distance $r < r_c = 2\sigma$, and 0 otherwise, $\kappa = 1\sigma$ is the screening length and its length of 1 nm corresponds to the Debye screening length at physiological conditions. $\epsilon_{\rm E}$ defines the effective strength of the electrostatic interactions and is the second control parameter we will explore, while q_i represents the sign of the charge of bead i ($q_i = \pm 1$). Since neighboring beads in a molecule have overlapping volume and distances between charges in the same molecule can be small, we exclude interactions of beads in the same molecule for 1-2, 1-3, 1-4, and 1-5 neighbors. The simulations are initialized by randomizing the positions and orientations of $N = 2500$ molecules in a cubic box of length $L = 171\sigma$, resulting in a molecule number concentration of $c_{\rm mol} = 0.0005\sigma^{-3}$. We integrate the system in the NVE ensemble (V, E being the volume of the box and the total energy of the system, respectively) with a Langevin thermostat to simulate Brownian motion of the molecules, with the LAMMPS MD package (87). Our integration timestep is $0.001\tau_0$, where τ_0 denotes the MD unit of time, and the damping coefficient was chosen to be $1\tau_0$.

ACKNOWLEDGEMENTS

We thank Dr. Steven Roeters (Aarhus University), Dr. Federica Burla, Prof. Dr. Nico Sommerdijk (Radboud Medical Center, Nijmegen, The Netherlands) and Prof.Dr. Mischa Bonn (Institute for Polymer Research, Mainz, Germany) for the useful discussion. We thank Dr. Wim Roeterdink and Michiel Hilberts for the technical support. GK acknowledges financial support by the "BaSyC - Building a Synthetic Cell" Gravitation grant (024.003.019) of The Netherlands Ministry of Education, Culture and Science (OCW) and The Netherlands Organization for Scientific Research and from NWO grant OCENW.GROOT.2019.022. This publication is part of the project (with Project Number VI.Veni.212.240) of the research programme NWO Talent Programme Veni 2021, which is financed by the Dutch Research Council (NWO). We acknowledge support from the Sectorplan Bèta & Techniek of the Dutch Government.

Bibliography

1. P. Fratzl. *Collagen: Structure and mechanics, an introduction*. Springer US, 2008. ISBN 9780387739052.
2. Matthew D Shoulders and Ronald T Raines. Collagen structure and stability. *Annual Review of Biochemistry*, 78:929–958, 2009.
3. Ruud A. Bank, Johan M. Tekoppele, Guus J. M. Janus, Maurice H. M. Wassen, Hans E. H. Pruijs, Hans A. H. van der Sluijs, and Ralph J. B. Sakkers. Pyridinium cross-links in bone of patients with osteogenesis imperfecta: Evidence of a normal intrafibrillar collagen packing. *Journal of Bone and Mineral Research*, 15(7):1330–1336, 2000.
4. Alfonso De Simone, Luigi Vitagliano, and Rita Berisio. Role of hydration in collagen triple helix stabilization. *Biochemical and Biophysical Research Communications*, 372:121–125, 7 2008.
5. Krishnakumar M. Ravikumar and Wonmuk Hwang. Region-specific role of water in collagen unwinding and assembly. *Proteins: Structure, Function, and Bioinformatics*, 72(4):1320–1332, 2008.
6. J Bella, M Eaton, B Brodsky, and H. Berman. Crystal and molecular structure of a collagen-like peptide at 1.9 Å resolution. *Science*, 266:75–81, 10 1994. ISSN 0036-8075.
7. Michele Cutini, Stefano Pantaleone, and Piero Ugliengo. Elucidating the nature of interactions in collagen triple-helix wrapping. *Journal of Physical Chemistry Letters*, 10(24):7644–7649, 2019.
8. Luigi Vitagliano, Rita Berisio, and Alfonso DeSimone. Role of hydration in collagen recognition by bacterial adhesins. *Biophysical Journal*, 100(9):2253–2261, 2011.
9. S. Leikin, V. A. Parsegian, W. H. Yang, and G. E. Walrafen. Raman spectral evidence for hydration forces between collagen triple helices. *Proceedings of the National Academy of Sciences of the United States of America*, 94:11312–11317, 10 1997.
10. S Leikin, D C Rau, and V A Parsegian. Direct measurement of forces between self-assembled proteins: temperature-dependent exponential forces between collagen triple helices. *Proceedings of the National Academy of Sciences*, 91(1):276–280, 1994.
11. Sergey Leikin, Donald Rau, and Vozken Parsegian. Temperature-favored assembly of collagen is driven by hydrophilic not hydrophobic interactions. *Nature Structural Biology*, 2:205–10, 04 1995.
12. N. Kuznetsova, D.C. Rau, V.A. Parsegian, and S. Leikin. Solvent hydrogen-bond network in protein self-assembly: solvation of collagen triple helices in nonaqueous solvents. *Biophysical Journal*, 72(1):353–362, 1997.
13. Michele Ceriotti, Wei Fang, Peter G. Kusalik, Ross H. McKenzie, Angelos Michaelides, Miguel A. Morales, and Thomas E. Markland. Nuclear quantum effects in water and aqueous systems: Experiment, theory, and current challenges. *Chemical Reviews*, 116:7529–7550, 7 2016.
14. George Némethy and Harold A. Scheraga. Structure of water and hydrophobic bonding in proteins. iv. the thermodynamic properties of liquid deuterium oxide. *Journal of Chemical Physics*, 41:680–689, 8 1964.
15. Lengwan Li, Jacek Jakowski, Changwoo Do, and Kunlun Hong. Deuteration and polymers: Rich history with great potential. *Macromolecules*, 54:3555–3584, 4 2021.
16. Amberley D. Stephens, Johanna Kölbel, Rani Moons, Chyi Wei Chung, Michael T. Ruggiero, Najet Mahmoudi, Talia A. Shmool, Thomas M. McCoy, Daniel Nietlispach, Alexander F. Routh, Frank Sobott, J. Axel Zeitler, and Gabriele S. Kaminski Schierle. Decreased water mobility contributes to increased α-synuclein aggregation. *Angewandte Chemie International Edition*, 62(7):e202212063, 2023.
17. S. Y. Chun, M. K. Son, C. R. Park, C. Lim, H. I. Kim, K. Kwak, and M. Cho. Direct observation of protein structural transitions through entire amyloid aggregation processes in water using 2D-IR spectroscopy. *Chem. Sci*, 13:4482–4489, 2022.
18. Jerome Gross and David Kirk. The heat precipitation of collagen from neutral salt solutions: Some rate-regulating factors. *Journal of Biological Chemistry*, 233(2):355–360, 1958. ISSN 0021-9258.
19. G. C. Wood and M. K. Keech. The formation of fibrils from collagen solutions 1. the effect of experimental conditions: Kinetic and electron-microscope studies. *Biochemical Journal*, 75(3):588–598, 06 1960. ISSN 0006-2936.

20. Jieling Zhu and Laura J. Kaufman. Collagen i self-assembly: Revealing the developing structures that generate turbidity. *Biophysical Journal*, 106(8):1822–1831, 2014. ISSN 0006-3495.
21. Frederick H. Silver and David E. Birk. Kinetic Analysis of Collagen Fibrillogenesis: I. Use of Turbidity-Time Data. *Collagen and Related Research*, 3(5):393–405, 1983. ISSN 0174-173X.
22. Karin A. Jansen, Albert J. Licup, Abhinav Sharma, Robbie Rens, Fred C. MacKintosh, and Gijsje H. Koenderink. The role of network architecture in collagen mechanics. *Biophysical Journal*, 114(11):2665–2678, 2018. ISSN 0006-3495.
23. Christopher Allen Rucksack Jones, Long Liang, Daniel Lin, Yang Jiao, and Bo Sun. The spatial-temporal characteristics of type I collagen-based extracellular matrix. *Soft Matter*, 10:8855–8863, 2014.
24. Kenji Okuyama, Keita Miyama, Kazunori Mizuno, and Hans Peter Bächinger. Crystal structure of $(Gly\text{-}Pro\text{-}Hyp)_9$:implications for the collagen molecular model. *Biopolymers*, 97: 607–616, 2012.
25. Smriti Mukherjee, Arun Gopinath, Balaraman Madhan, and Ganesh Shanmugam. Vibrational circular dichroism spectroscopy as a probe for the detection of collagen fibril and fibrillation in solution. *Biosensors and Bioelectronics: X*, 10:100108, 2022.
26. Andreas Barth and Christian Zscherp. What vibrations tell us about proteins. *Quarterly Reviews of Biophysics*, 35:369–430, 11 2002.
27. P.Hamm and M.Zanni. *Concepts and Methods of 2D Infrared Spectroscopy*. Cambridge University Press, 2011.
28. Sachin Kumar, Yujen Wang, Mohammadhasan Hedayati, Frederik Fleissner, Manuel K Rausch, and Sapun H Parekh. Structural control of fibrin bioactivity by mechanical deformation. *Proceedings of the National Academy of Sciences*, 119(22):e2117675119, 2022.
29. Rajendra S. Bhatnagar and Craig A. Gough. *Circular Dichroism of Collagen and Related Polypeptides*. Springer US, 1996.
30. Eesha Khare, Chi-Hua Yu, Constancio Gonzalez Obeso, Mario Milazzo, David L. Kaplan, and Markus J. Buehler. Discovering design principles of collagen molecular stability using a genetic algorithm, deep learning, and experimental validation. *Proceedings of the National Academy of Sciences*, 119(40):e2209524119, 2022.
31. Kazunori Mizuno and Hans Peter Bächinger. The effect of deuterium oxide on the stability of the collagen model peptides $H\text{-}(Pro\text{-}Pro\text{-}Gly)_{10}\text{-}OH$, $H\text{-}(Gly\text{-}Pro\text{-}4(R)Hyp)_9\text{-}OH$, and Type I collagen. *Biopolymers*, 93:93–101, 1 2010. ISSN 00063525.
32. Anne George and Arthur Veis. FTIR in water demonstrates that collagen monomers undergo a conformational transition prior to thermal self-assembly in vitro. *Biochemistry*, 30 (9):2372–2377, 1991.
33. R. J. Jakobsen, L. L. Brown, T. B. Hutson, D. J. Fink, and A. Veis. Intermolecular interactions in collagen self-assembly as revealed by fourier transform infrared spectroscopy. *Science*, 220(4603):1288–1290, 1983.
34. Yu A Lazarev, BA Grishkovsky, and TB Khromova. Amide I band of IR spectrum and structure of collagen and related polypeptides. *Biopolymers: Original Research on Biomolecules*, 24(8):1449–1478, 1985.
35. Qi Guo, Philip Pagano, Yun-Liang Li, Amnon Kohen, and Christopher M. Cheatum. Line shape analysis of two-dimensional infrared spectra. *Journal of Chemical Physics*, 142(21): 212427, 2015.
36. Rita Guzzi, Caterina Arcangeli, and Anna Rita Bizzarri. A molecular dynamics simulation study of the solvent isotope effect on copper plastocyanin. *Biophysical Chemistry*, 82:9–22, 11 1999. ISSN 03014622.
37. Sheh-Yi Sheu, E. W. Schlag, H. L. Selzle, and Dah-Yen Yang. Molecular Dynamics of Hydrogen Bonds in Protein-D_2O: The Solvent Isotope Effect. *Journal of Physical Chemistry A*, 112:797–802, 2 2008.
38. George C. Na, Linda J. Phillips, and Ernesto I. Freire. In vitro collagen fibril assembly: thermodynamic studies. *Biochemistry*, 28(18):7153–7161, 1989.
39. Svetlana Morozova and Murugappan Muthukumar. Electrostatic effects in collagen fibril formation. *Journal of Chemical Physics*, 149(16):163333, 2018.
40. Frederick H. Silver. A molecular model for linear and lateral growth of type i collagen fibrils. *Collagen and Related Research*, 2(3):219–229, 1982.
41. Ludovica Leo, Maria Grazia Bridelli, and Eugenia Polverini. Insight on collagen self-assembly mechanisms by coupling molecular dynamics and uv spectroscopy techniques. *Biophysical Chemistry*, 253:106224, 2019.
42. Ian Streeter and Nora H. de Leeuw. A molecular dynamics study of the interprotein interactions in collagen fibrils. *Soft Matter*, 7:3373–3382, 2011.
43. Rita Berisio, Luigi Vitagliano, Lelio Mazzarella, and Adriana Zagari. Crystal structure of a collagen-like polypeptide with repeating sequence pro–hyp–gly at 1.4 Å resolution: Implications for collagen hydration. *Biopolymers*, 56(1):8–13, 2000.
44. Martijn de Wild, Wim Pomp, and Gijsje H. Koenderink. Thermal memory in self-assembled collagen fibril networks. *Biophysical Journal*, 105(1):200–210, 2013. ISSN 0006-3495.
45. Andrew R. McCluskey, Kennes S. W. Hung, Bartosz Marzec, Julien O. Sindt, Nico A. J. M. Sommerdijk, Philip J. Camp, and Fabio Nudelman. Disordered filaments mediate the fibrillogenesis of type i collagen in solution. *Biomacromolecules*, 21(9):3631–3643, 2020.
46. Anne E. Hafner, Noemi G. Gyori, Ciaran A. Bench, Luke K. Davis, and Anđela Šarić. Modeling fibrillogenesis of collagen-mimetic molecules. *Biophysical Journal*, 119(9):1791–1799, 2020.
47. G. C. Wood. The formation of fibrils from collagen solutions. 2. A mechanism for collagen-fibril formation. *Biochemical Journal*, 75(3):598–605, 06 1960.
48. Carmelo Tempra, Victor Cruces Chamorro, and Pavel Jungwirth. Effects of water deuteration on thermodynamic and structural properties of proteins and biomembranes. *Journal of Physical Chemistry B*, 127(5):1138–1143, 2023.
49. Natalie Ben Abu, Philip E Mason, Hadar Klein, Nitzan Dubovski, Yaron Ben Shoshan-Galeczki, Einav Malach, Veronika Pražienková, Lenka Maletínská, Carmelo Tempra, Victor Cruces Chamorro, Josef Cvačka, Maik Behrens, Masha Y. Niv, and Pavel Jungwirth. Sweet taste of heavy water. *Communications Biology*, 4:440, 12 2021. ISSN 2399-3642.
50. B. Wierczinski W. Norde A. A. van Well Y. M. Efimova, S. Haemers. Stability of globular proteins in H_2O and D_2O. *Biopolymers*, 85:264–273, 2 2007. ISSN 00063525.
51. Mouhamad Reslan and Veysel Kayser. The effect of deuterium oxide on the conformational stability and aggregation of bovine serum albumin. *Pharmaceutical Development and Technology*, 23:1030–1036, 11 2018.
52. Yang Zhou and Daiwen Yang. Equilibrium folding dynamics of meacp in water, heavy water, and low concentration of urea. *Scientific Reports*, 7:16156, 12 2017. ISSN 2045-2322. doi: 10.1038/s41598-017-16449-4.
53. Arup K. Pathak and Tusar Bandyopadhyay. Water isotope effect on the thermostability of a polio viral rna hairpin: A metadynamics study. *Journal of Chemical Physics*, 146:165104, 4 2017.
54. Marcus Vinícius Cangussu Cardoso and Edvaldo Sabadini. The gelling of κ-carrageenan in light and heavy water. *Carbohydrate Research*, 345:2368–2373, 11 2010. ISSN 00086215.
55. Samantha S. Stadmiller and Gary J. Pielak. Enthalpic stabilization of an SH3 domain by D_2O. *Protein Science*, 27:1710–1716, 9 2018. ISSN 0961-8368.
56. Patrizia Cioni and Giovanni B. Strambini. Effect of heavy water on protein flexibility. *Biophysical Journal*, 82:3246–3253, 6 2002. ISSN 00063495.
57. Brian W. Chellgren and Trevor P. Creamer. Effects of H_2O and D_2O on polyproline ii helical structure. *Journal of the American Chemical Society*, 126:14734–14735, 11 2004.
58. Jörg Schnauß, Tom Kunschmann, Steffen Grosser, Paul Mollenkopf, Tobias Zech, Jessica S. Freitag, Dusan Prascevic, Roland Stange, Luisa S. Röttger, Susanne Rönicke, David M. Smith, Thomas M. Bayerl, and Josef A. Käs. Cells in slow motion: Apparent undercooling increases glassy behavior at physiological temperatures. *Advanced Materials*, 33(29):2101840, 2021.
59. José D. Camino, Pablo Gracia, and Nunilo Cremades. The role of water in the primary nucleation of protein amyloid aggregation. *Biophysical Chemistry*, 269:106520, 2021. ISSN 0301-4622. doi: https://doi.org/10.1016/j.bpc.2020.106520.
60. Bogdan Tarus, John E. Straub, and D. Thirumalai. Dynamics of asp23-lys28 salt-bridge formation in aβ10-35 monomers. *Journal of the American Chemical Society*, 128(50):16159–16168, 2006.
61. Yan Wang, Thierry Azaïs, Marc Robin, Anne Vallée, Chelsea Catania, Patrick Legriel, Gérard Pehau-Arnaudet, Florence Babonneau, Marie-Madeleine Giraud-Guille, and Nadine Nassif. The predominant role of collagen in the nucleation, growth, structure and orientation of bone apatite. *Nature materials*, 11 8, 2012.
62. Federica Burla, Justin Tauber, Simone Dussi, Jasper Gucht, and Gijsje Koenderink. Stress management in composite biopolymer networks. *Nature Physics*, 15, 02 2019.
63. Luca Bertinetti, Admir Masic, Roman Schuetz, Aurelio Barbetta, Britta Seidt, Wolfgang Wagermaier, and Peter Fratzl. Osmotically driven tensile stress in collagen-based mineralized tissues. *Journal of the Mechanical Behavior of Biomedical Materials*, 52:14–21, 2015.
64. Rachel K. Surowiec, Matthew R. Allen, and Joseph M. Wallace. Bone hydration: How we can evaluate it, what can it tell us, and is it an effective therapeutic target? *Bone Reports*, 16:101161, 2022.
65. O. G. Andriotis, S. W. Chang, M. Vanleene, P. H. Howarth, D. E. Davies, S. J. Shefelbine, M. J. Buehler, and P. J. Thurner. Structure–mechanics relationships of collagen fibrils in the osteogenesis imperfecta mouse model. *Journal of The Royal Society Interface*, 12: 20150701, 10 2015.
66. Orestis G. Andriotis, Kareem Elsayad, David E. Smart, Mathis Nalbach, Donna E. Davies, and Philipp J. Thurner. Hydration and nanomechanical changes in collagen fibrils bearing advanced glycation end-products. *Biomed. Opt. Express*, 10(4):1841–1855, Apr 2019.
67. Lauria Claeys, Silvia Storoni, Marelise Eekhoff, Mariet Elting, Lisanne Wisse, Gerard Pals, Nathalie Bravenboer, Alessandra Maugeri, and Dimitra Micha. Collagen transport and related pathways in osteogenesis imperfecta. *Human Genetics*, 140, 2021.
68. Fransiska Malfait, Clair Francomano, Peter Byers, John Belmont, Britta Berglund, James Black, Lara Bloom, Jessica M. Bowen, Angela F. Brady, Nigel P. Burrows, Marco Castori, Helen Cohen, Marina Colombi, Serwet Demirdas, Julie De Backer, Anne De Paepe, Sylvie Fournel-Gigleux, Michael Frank, Neeti Ghali, Cecilia Giunta, Rodney Grahame, Alan Hakim, Xavier Jeunemaitre, Diana Johnson, Birgit Juul-Kristensen, Ines Kapferer-Seebacher, Hanadi Kazkaz, Tomoki Kosho, Mark E. Lavallee, Howard Levy, Roberto Mendoza-Londono, Melanie Pepin, F. Michael Pope, Eyal Reinstein, Leema Robert, Marianne Rohrbach, Lynn Sanders, Glenda J. Sobey, Tim Van Damme, Anthony Vandersteen, Caroline van Mourik, Nicol Voermans, Nigel Wheeldon, Johannes Zschocke, and Brad Tinkle. The 2017 international classification of the ehlers–danlos syndromes. *American Journal of Medical Genetics Part C: Seminars in Medical Genetics*, 175(1):8–26, 2017.
69. Francis H. Glorieux. Caffey disease: an unlikely collagenopathy. *Journal of Clinical Investigation*, 115, 5 2005.
70. P.H. Byers, G.A. Wallis, and M.C. Willing. Osteogenesis imperfecta: translation of mutation to phenotype. *Journal of Medical Genetics*, 28(7):433–442, 1991.
71. Julian Hartmann and Martin Zacharias. Mechanism of collagen folding propagation studied by molecular dynamics simulations. *PLOS Computational Biology*, 17, 06 2021.
72. J.P. Cassella, P. Barber, A.C. Catterall, and S.Yousuf Ali. A morphometric analysis of osteoid collagen fibril diameter in osteogenesis imperfecta. *Bone*, 15(3):329–334, 1994.
73. Maxime A. Gallant, Drew M. Brown, Max Hammond, Joseph M. Wallace, Jiang Du, Alix C. Deymier-Black, Jonathan D. Almer, Stuart R. Stock, Matthew R. Allen, and David B. Burr. Bone cell-independent benefits of raloxifene on the skeleton: A novel mechanism for improving bone material properties. *Bone*, 61:191–200, 2014.
74. Artur Krężel and Wojciech Bal. A formula for correlating pka values determined in D_2O and H_2O. *Journal of Inorganic Biochemistry*, 98(1):161–166, 2004.
75. Adriana Huerta-Viga, Daniel J. Shaw, and Sander Woutersen. ph dependence of the conformation of small peptides investigated with two-dimensional vibrational spectroscopy. *Journal of Physical Chemistry B*, 114:15212–15220, 11 2010. doi: 10.1021/JP105133R.
76. Cristina Martinez-Torres, Federica Burla, Celine Alkemade, and Gijsje H. Koenderink. Revealing the assembly of filamentous proteins with scanning transmission electron microscopy. *PLOS ONE*, 14:1–16, 12 2019.
77. Caroline A Schneider, Wayne S Rasband, and Kevin W Eliceiri. NIH Image to ImageJ: 25 years of image analysis. *Nature methods*, 9(7):671–675, 2012.
78. Herman JC Berendsen, David van der Spoel, and Rudi van Drunen. Gromacs: a message-passing parallel molecular dynamics implementation. *Comput. Phys. Commun.*, 91:43–56, 1995.
79. Berk Hess, Carsten Kutzner, David Van Der Spoel, and Erik Lindahl. Gromacs 4: al-

gorithms for highly efficient, load-balanced, and scalable molecular simulation. *J. Chem. Theor. Comp.*, 4(3):435–447, 2008.

80. Jing Huang, Sarah Rauscher, Grzegorz Nawrocki, Ting Ran, Michael Feig, Bert L De Groot, Helmut Grubmüller, and Alexander D MacKerell. Charm36m: an improved force field for folded and intrinsically disordered proteins. *Nat. Met.*, 14:71–73, 2017.
81. Johanna-Barbara Linse and Jochen S Hub. Three- and four-site models for heavy water: Spc/e-hw, tip3p-hw, and tip4p/2005-hw. *J. Chem. Phys.*, 154:195401, 2021.
82. William L Jorgensen, Jayaraman Chandrasekhar, Jeffry D Madura, Roger W Impey, and Michael L Klein. Comparison of simple potential functions for simulating liquid water. *J. Chem. Phys.*, 79:926–935, 1983.
83. Giovanni Bussi, Davide Donadio, and Michele Parrinello. Canonical sampling through velocity rescaling. *J. Chem. Phys.*, 126(1):014101, 2007.
84. Herman JC Berendsen, JPM van Postma, Wilfred F Van Gunsteren, ARHJ DiNola, and Jan R Haak. Molecular dynamics with coupling to an external bath. *J. Chem. Phys.*, 81: 3684–3690, 1984.
85. Tom Darden, Darrin York, and Lee Pedersen. Particle mesh Ewald: an Nlog(N) method for Ewald sums in large systems. *J. Chem. Phys.*, 98(12):10089–10092, 1993.
86. Shyam Rele, Yuhua Song, Robert P. Apkarian, Zheng Qu, Vincent P. Conticello, and Elliot L. Chaikof. D-periodic collagen-mimetic microfibers. *Journal of the American Chemical Society*, 129(47):14780–14787, 2007.
87. A. P. Thompson, H. M. Aktulga, R. Berger, D. S. Bolintineanu, W. M. Brown, P. S. Crozier, P. J. in 't Veld, A. Kohlmeyer, S. G. Moore, T. D. Nguyen, R. Shan, M. J. Stevens, J. Tranchida, C. Trott, and S. J. Plimpton. LAMMPS - a flexible simulation tool for particle-based materials modeling at the atomic, meso, and continuum scales. *Comp. Phys. Comm.*, 271:108171, 2022.